

STRATIFICATION OF SUNSPOT UMBRAL DOTS FROM INVERSION OF STOKES PROFILES RECORDED BY *Hinode*

T. L. RIETHMÜLLER, S. K. SOLANKI, AND A. LAGG

Max-Planck-Institut für Sonnensystemforschung, Max-Planck-Strasse 2, 37191 Katlenburg-Lindau, Germany;

riethmueller@mps.mpg.de, solanki@mps.mpg.de, lagg@mps.mpg.de

Received 2008 March 12; accepted 2008 March 28; published 2008 April 21

ABSTRACT

This work aims to constrain the physical nature of umbral dots (UDs) using high-resolution spectropolarimetry. Full Stokes spectra recorded by the spectropolarimeter on *Hinode* of 51 UD's in a sunspot close to the disk center are analyzed. The height dependence of the temperature, magnetic field vector, and line-of-sight velocity across each UD is obtained from an inversion of the Stokes vectors of the two Fe I lines at 630 nm. No difference is found at higher altitudes [$-3 \leq \log(\tau_{500}) \leq -2$] between the UD's and the diffuse umbral background. Below that level the difference rapidly increases, so that at the continuum formation level [$\log(\tau_{500}) = 0$] we find on average a temperature enhancement of 570 K, a magnetic field weakening of 510 G, and upflows of 800 m s⁻¹ for peripheral UD's, whereas central UD's display an excess temperature of on average 550 K, a field weakening of 480 G, and no significant upflows. The results for, in particular, the peripheral UD's, including cuts of magnetic vector and velocity through them, look remarkably similar to the output of recent radiation MHD simulations. They strongly suggest that UD's are produced by convective upwellings.

Subject headings: Sun: photosphere — sunspots — techniques: spectroscopic

Online material: color figures

1. INTRODUCTION

The energy transport immediately below the solar surface is mainly determined by convective processes that are visible as granulation patterns in white-light images of the quiet photosphere. This convection is suppressed inside sunspot umbrae due to the strong vertical magnetic field, but some form of magnetoconvection (Weiss 2002) is needed to explain the observed umbral brightnesses. Umbral fine structure such as light bridges or umbral dots, dotlike bright features inside umbrae, may well be manifestations of magnetoconvection. Different models have been proposed to explain UD's, e.g., columns of field-free hot gas in between a bundle of thin magnetic flux ropes (Parker 1979; Choudhury 1986), or spatially modulated oscillations in a strong magnetic field (Weiss et al. 1990). Recent numerical simulations of three-dimensional radiative magnetoconvection (Schüssler & Vögler 2006) reveal convective plumes that penetrate through the solar surface and look very much like UD's. Although recent broadband images may have spatially resolved UD's (Sobotka & Hanslmeier 2005; T. L. Riethmüller et al. 2008, in preparation), spectropolarimetry is needed to learn more about their physical nature. Previous spectroscopic observations led to heterogeneous results. Kneer (1973) found that UD's exhibit upflows of 3 km s⁻¹ and a 50% weaker magnetic field compared to the nearby umbra, whereas Lites et al. (1991) and Tritschler & Schmidt (1997) reported little field weakening. Finally, Socas-Navarro et al. (2004) observed a weakening of 500 G and upflows of a few 100 m s⁻¹. More details can be found in the reviews of umbral fine structure by Solanki (2003) and Sobotka (2006). One reason for the difference in results has been the influence of scattered light and variable seeing, which affect the different analyzed data sets to varying degrees. It therefore seems worthwhile to invert Stokes profiles obtained by the spectropolarimeter (SP) on the *Hinode* spacecraft. The usefulness of *Hinode* data for the study of UD's was demonstrated by Bharti et al. (2007) who found that large UD's show dark lanes whose existence had been predicted by Schüssler & Vögler (2006).

2. OBSERVATIONS AND DATA REDUCTION

The data employed here were acquired by the spectropolarimeter (Lites et al. 2001) of the Solar Optical Telescope (SOT; Suematsu et al. 2008) on board *Hinode*. They are composed of full Stokes spectra in the Fe I line pair around 6302 Å and the nearby continuum of a sunspot of NOAA AR 10933 recorded from 12:43 to 12:59 UT on 2007 January 5 using the 0.16" × 164" slit. At this time the sunspot was located at a heliocentric angle of 4°, i.e., very close to disk center. The observations covered the spectral range from 6300.89 to 6303.26 Å, with a sampling of 21 mÅ pixel⁻¹. The SP was operated in its normal map mode, i.e., both the sampling along the slit and the slit-scan sampling were 0.16", so that the spatial resolution should be close to the diffraction limit of 1.22λ/D = 0.32". The integration time per slit position was 4.8 s which reduced the noise level to 10⁻³I_c.

The data were corrected for dark current, flat field, and instrumental polarization with the help of the SolarSoft package.¹ A continuum intensity image (put together from the slit scan) of the chosen umbra is shown in Figure 1. Due to the large slit length we are always able to find a sufficiently extensive region of quiet Sun that is used to normalize intensities.

3. DATA ANALYSIS

To obtain atmospheric stratifications of temperature (T), magnetic field strength (B), and line-of-sight velocity (v_{LOS}) we use the inversion code SPINOR described by Frutiger et al. (2000). This code incorporates the STOPRO routines (Solanki 1987), which compute synthetic Stokes profiles of one or more lines upon input of their atomic data and one or more model atmospheres. Local thermodynamic equilibrium conditions are assumed and the Unno-Rachkovsky radiative transfer equations are solved. The inversions use an optical depth scale as the appropriate coordinate for radiative transfer problems. For rea-

¹ See <http://www.lmsal.com/solarsoft>.

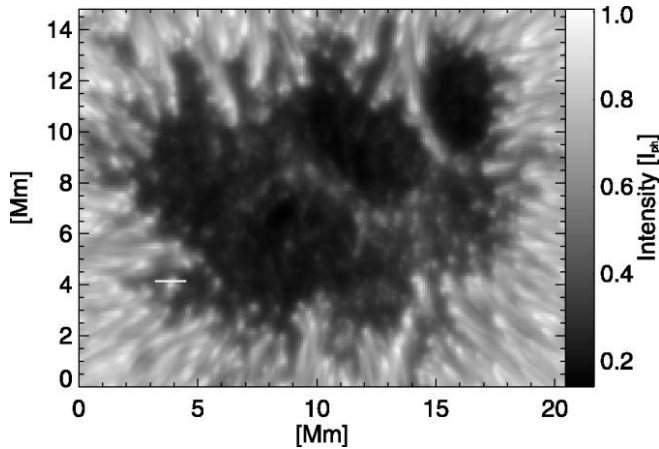


FIG. 1.—Continuum intensity map of the sunspot AR 10933 as observed by the *Hinode* SOT/SP on 2007 January 5. Heliocentric angle is $\theta = 4^\circ$. Intensities are normalized to the intensity level of the quiet photosphere I_{ph} . The white line at (4, 4) Mm marks the cut through an umbra dot (UD) that is discussed in greater detail.

sons of comparability we use the optical depth at 500 nm (τ_{500}). Starting with an initial guess model, the synthetic profiles were iteratively fitted to observed data using response functions (RFs) and the merit function χ^2 (Ruiz Cobo & del Toro Iniesta 1992; Frutiger 2000) is minimized. With the help of the RFs we find that the Fe I line pair at 6302 Å is mainly formed within the $\log(\tau_{500})$ interval $[-3, 0]$, which corresponds to a height range of about 400 km under hydrostatic equilibrium conditions in the umbra. The free parameters are defined at the four nodes $-3, -2, -1, \text{ and } 0$ of the $\log(\tau_{500})$ grid. The atmospheric stratification is then interpolated using splines onto a 10 times finer $\log(\tau_{500})$ grid.

The first step of our analysis is the wavelength calibration required to determine line-of-sight (LOS) velocities. For every slit position we average the Stokes I profiles of all locations along the slit whose total polarization $P = \int (Q^2 + U^2 + V^2)^{1/2} d\lambda$ is negligible, since those locations are assumed to represent the quiet Sun. This mean I profile is used to fit Voigt profiles to the two Fe I lines from which the line-center wavelengths are determined. The convective blueshift of 140 m s^{-1} (see Martínez Pillet et al. 1997; Dravins et al. 1981) is then removed.

The next step is to find an appropriate model atmosphere. Since we are interested in the atmospheric stratification of temperature, magnetic field strength, and LOS velocity within an UD, these three atmospheric parameters are assumed to be height dependent, whereas field inclination and azimuth angle, microturbulence, and macroturbulence are assumed to be height independent. We experimented intensively with adding a second model component to represent the stray light, but the inversion results did not improve significantly, confirming the almost negligible stray light in the SP. Therefore, in the interests of a robust inversion, we forbore from adding a stray-light component, thus reducing the number of free parameters.

Lastly, we have to find initial guesses for all free parameters. We use an initial temperature stratification according to the umbra core model L of Maltby et al. (1986) and assume a vertical magnetic field of 2000 G and zero LOS velocity at all heights. Initial guesses for microturbulence and macroturbulence are 0.1 and 2 km s^{-1} , respectively. Other initial guesses gave very similar results, except for a limited number of outliers. For these, repeating the inversion with an initial guess

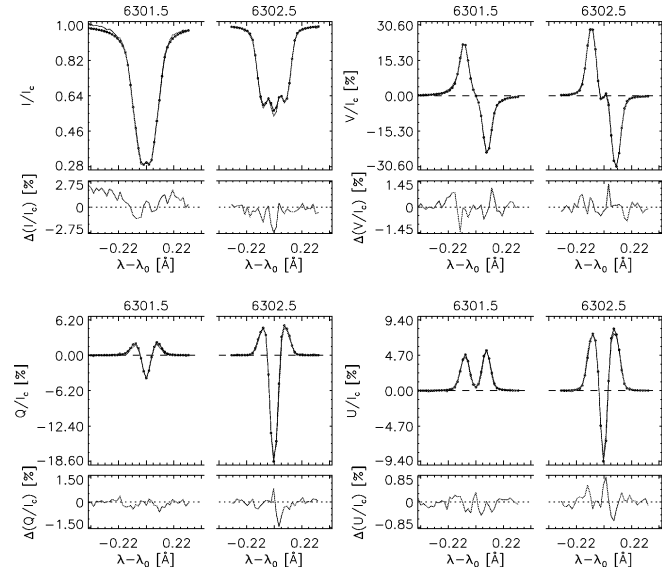


FIG. 2.—Stokes $I, V, Q,$ and U profiles from the center of the UD marked in Fig. 1. Lighter lines are the measured, darker lines the best-fit profiles, i.e., the inversion result. The bottom parts of each panel show the difference between the two on an expanded scale. [See the electronic edition of the *Journal* for a color version of this figure.]

close to the final result of one of the neighboring pixels returned values consistent with those obtained for the other pixels.

4. INVERSION RESULTS

We analyzed a total of 51 UD, which were identified by applying the multilevel tracking (MLT) algorithm (Bovelet & Wiehr 2001; T. L. Riethmüller et al. 2008, in preparation). For each UD the location of its core was identified, a cut was made through it, reaching to the neighboring diffuse background (DB), and the profiles from all the pixels along this cut were inverted. We first discuss the results for the UD marked in Figure 1, chosen because of its brightness, which leads to particularly small error bars. A comparison of the measured profiles with the best-fit profiles resulted from the inversion can be seen in Figure 2 for the UD and in Figure 3 for the DB selected as the location of lowest continuum intensity in a $1.4 \times 1.4 \text{ Mm}^2$ environment of the UD center. Due to the low signal in the dark background the measured DB profiles are much noisier than the UD center's profiles, but in general, the Stokes spectra can be fitted remarkably well.

The stratification of the retrieved atmospheric parameters $T, v_{\text{LOS}},$ and B in the center of the UD and in the DB are plotted in Figure 4. In the upper photosphere $[-3 \leq \log(\tau_{500}) \leq -2]$ the error bars overlap; i.e., we find little significant difference between UD and DB. In the deeper photosphere, however, the inversions return strongly different stratifications. Thus, the UD temperature is higher than the DB temperature, consistent with the intensity enhancement of the UD in the continuum map. The LOS velocity (which is identical to the vertical velocity due to the small heliocentric angle) exhibits strong upflows in the UD center, whereas the DB is nearly at rest. The magnetic field strength is roughly 2 kG for the heights $-3 \leq \log(\tau_{500}) \leq -1$. Below $\log(\tau_{500}) = -1$ the field strength of the UD decreases strongly with depth, whereas the field strength of the DB increases moderately.

The vertical cuts of magnetic field strength and LOS velocity through 13 pixels lying along the white line in Figure 1 are

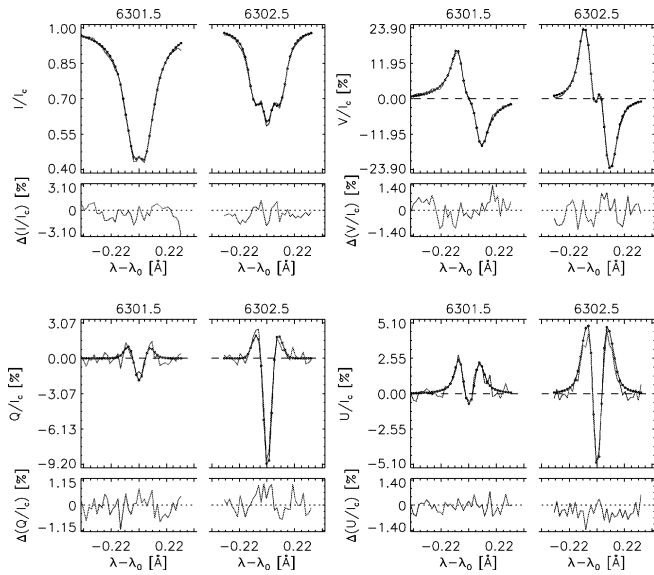


FIG. 3.—Same as Fig. 2, but for Stokes I , V , Q , and U profiles of the diffuse background near the UD. [See the electronic edition of the Journal for a color version of this figure.]

shown in Figure 5. Jumps from one pixel to the next were smoothed through interpolation. There is clear evidence for a localized decrease in UD field strength in the low photosphere, collocated with an upflow that extends higher into the atmosphere and a weak downflow on at least one side. The magnetic fields are 4° more inclined in the UD than they are in the DB around the UD. Figure 5 looks remarkably like Figure 2 of Schüssler & Vögler (2006) in spite of the fact that Figure 5 is plotted on an optical depth scale in the vertical direction and is thus distorted by an unknown amount relative to a corresponding figure on a geometrical scale.

Next we discuss all 51 analyzed UDs. In the literature we often find a separation into two UD regimes. For example, Grossmann-Doerth et al. (1986) differentiate between peripheral UDs (PUDs) and central UDs (CUDs), i.e., between UDs that are born close to the umbra-penumbra boundary and UDs that are born deep in the umbra. We follow this distinction and plot the obtained stratifications of the 30 PUDs (distance to umbra-penumbra boundary less than 2000 km) in the top panels of Figure 6, while the remaining 21 CUDs are represented in the bottom panels of Figure 6. The results largely mirror those obtained for the UD discussed above. In the upper atmosphere UDs center and DB do not differ in their mean values of T , v_{LOS} , and B . On average, the CUDs are about 150 K cooler than the PUDs in the upper atmosphere, just as the DB around the CUDs is cooler than the DB around the PUDs. At $\log(\tau_{500}) = 0$ we find that PUDs are 570 K hotter than the local DB and CUDs are 550 K hotter than the DB in their vicinity. The magnetic field strength at $\log(\tau_{500}) = 0$ is weakened by about 510 G for PUDs and 480 G for CUDs, whereas only PUDs exhibit significant upflows of about 800 m s^{-1} . The mean LOS velocity shows no difference between CUD centers and DB. In order to make sure that an upflow is not being missed due to the lower S/N ratio of the CUD Stokes profiles, we have also averaged the Stokes profiles of all the CUDs. An inversion of these averaged Stokes profiles gave a result that agrees with the averaged stratifications (*thick dark line*) in the bottom panels of Figure 6 within the error bars. This suggests that any upflow velocity in CUDs is mostly restricted to layers

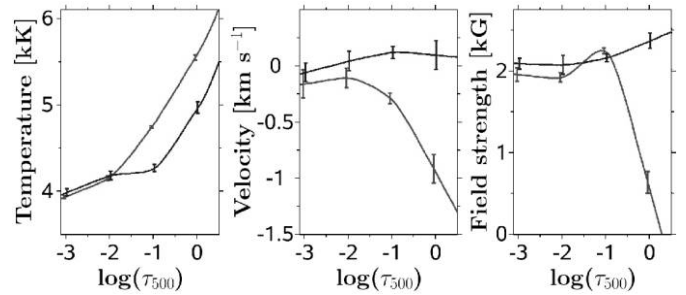


FIG. 4.—Atmospheric stratification obtained from the Stokes profiles at the location of the UD's center (*lighter lines*) and from the Stokes profiles of the diffuse background near the UD (*darker lines*). The formal errors of the inversion at the used optical depth nodes are indicated by bars. Negative LOS velocity values indicate upflows. [See the electronic edition of the Journal for a color version of this figure.]

below the surface or is too concentrated or too weak to be detected by the inversions. Finally, we find that the magnetic field of the PUDs is on average 4° more horizontal than for their DB. We see no inclination difference for CUDs.

5. DISCUSSION

We identified 30 peripheral and 21 central umbral dots in *Hinode* spectropolarimetric data of a sunspot within 4° of disk center. With the help of Stokes profile inversions of the Fe I

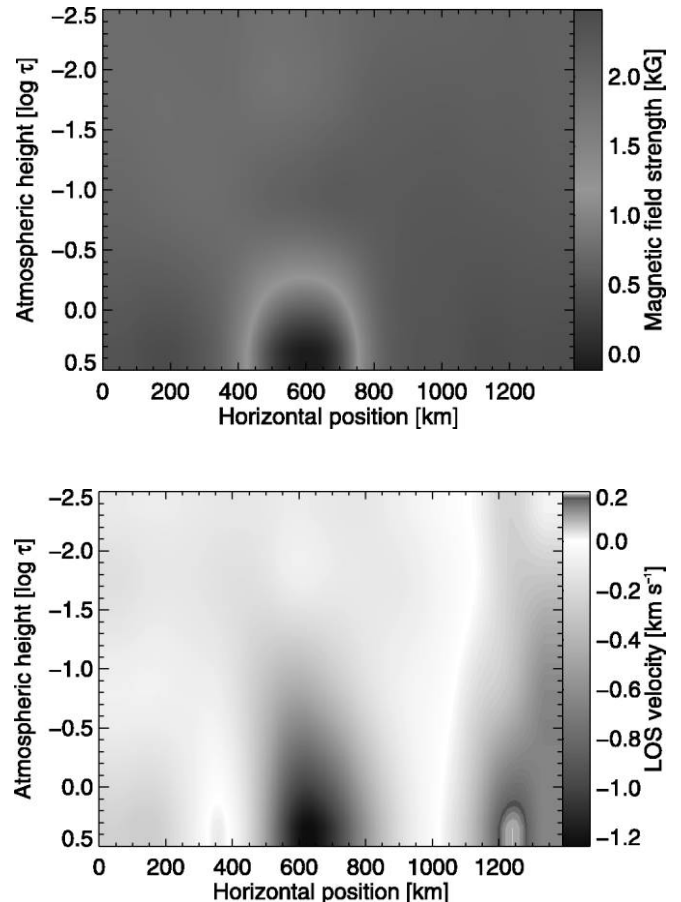


FIG. 5.—Vertical cut through the UD marked in Fig. 1 in the direction indicated by the white line. Colors of the top panel indicate magnetic field strength. The bottom panel shows LOS velocity. Negative velocities are upflows. [See the electronic edition of the Journal for a color version of this figure.]

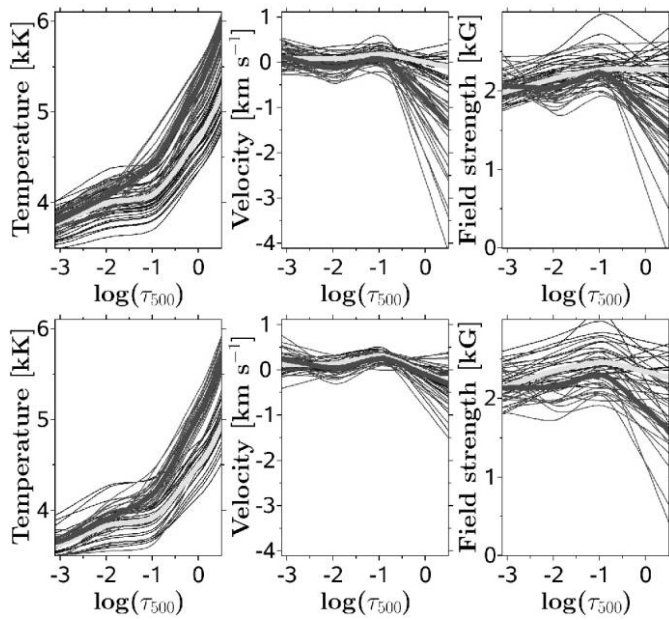


FIG. 6.—Atmospheric stratifications of peripheral umbral dots (*top three panels*) and central umbral dots (*bottom three panels*). The lighter thin lines show the stratification at the location of the UD's center and the darker thin lines correspond to the nearby diffuse background. The thick dark line is the weighted average of all lighter lines and the thick light line is the weighted average of all darker lines, where we used the reciprocal error bars as weighting factors. [See the electronic edition of the *Journal* for a color version of this figure.]

lines at 630 nm we determined the stratifications of temperature, magnetic field strength, and LOS velocity. The present work differs from that of Socas-Navarro et al. (2004) in the superior quality of the employed data with twice the spatial resolution and practically no scattered light. This allows a detailed de-

termination of the atmospheric stratification. The higher spatial resolution of the *Hinode* SP data also allows us to, for the first time, reconstruct both the horizontal and the vertical structure of UDs. We also extended the analysis to a more numerous statistical ensemble of 51 UDs.

Vertical cuts through UDs provide a remarkable confirmation of the results of MHD simulations of Schüssler & Vögler (2006): both show that UDs differ from their surroundings mainly in the lowest visible layers, where the temperature is enhanced and the magnetic field is weakened. We found a temperature enhancement of 550 K and a magnetic field reduction of about 500 G (at optical depth unity). In addition, PUDs display upflow velocities of 800 m s^{-1} on average, again in good agreement with the simulations. There are also some differences between our results and those of Schüssler & Vögler (2006). Thus, according to our inversions the magnetic field strength of the DB is somewhat depth dependent. This was not the case for the MHD simulations due to the used periodic boundary conditions. Furthermore, although some of the UDs display a weak downflow bounding the strong central upflow (see Fig. 5), these are neither as narrow nor as strong as the downflows at the ends of dark lanes as reported by Schüssler & Vögler (2006) probably due to the limited spatial resolution of our data. We may also be missing some of the narrow downflows by considering only single cuts across individual UDs.

Socas-Navarro et al. (2004) reported 10° more inclined magnetic fields in PUDs. This result is qualitatively confirmed by our work; we find an inclination increase of 4° for PUDs but no increase for CUDs, which can be assumed as a further hint that the main part of the CUD structure is below the surface. These results can be interpreted in terms of the strong DB fields expanding with height and closing over the UD, as proposed by Socas-Navarro et al. (2004).

REFERENCES

- Bharti, L., Joshi, C., & Jaaffrey, S. N. A. 2007, *ApJ*, 669, L57
 Bovelet, B., & Wiehr, E. 2001, *Sol. Phys.*, 201, 13
 Choudhury, A. R. 1986, *ApJ*, 302, 809
 Dravins, D., Lindegren, L., & Nordlund, Å. 1981, *A&A*, 96, 345
 Frutiger, C. 2000, Ph.D. thesis, Inst. Astron., ETH Zürich
 Frutiger, C., Solanki, S. K., Fligge, M., & Bruls, J. H. M. J. 2000, *A&A*, 358, 1109
 Grossmann-Doerth, U., Schmidt, W., & Schröter, E. H. 1986, *A&A*, 156, 347
 Kneer, F. 1973, *Sol. Phys.*, 28, 361
 Lites, B. W., Bida, T. A., Johannesson, A., & Scharmer, G. B. 1991, *ApJ*, 373, 683
 Lites, B. W., Elmore, D. F., & Stander, K. V. 2001, in *ASP Conf. Ser. 236, Advanced Solar Polarimetry*, ed. M. Sigwarth (San Francisco: ASP), 33
 Maltby, P., Avrett, E. H., Carlsson, M., Kjeldseth-Moe, O., Kurucz, R. L., & Loeser, R. 1986, *ApJ*, 306, 284
 Martínez Pillet, V., Lites, B. W., & Skumanich, A. 1997, *ApJ*, 474, 810
 Parker, E. N. 1979, *ApJ*, 234, 333
 Ruiz Cobo, B., & del Toro Iniesta, J. C. 1992, *ApJ*, 398, 375
 Schüssler, M., & Vögler, M. 2006, *ApJ*, 641, L73
 Sobotka, M. 2006, Diss. Doctor Scientiarum, Acad. Sci. Czech Republic
 Sobotka, M., & Hanslmeier, A. 2005, *A&A*, 442, 323
 Socas-Navarro, H., Martínez Pillet, V., Sobotka, M., & Vázquez, M. 2004, *ApJ*, 614, 448
 Solanki, S. K. 1987, Ph.D. thesis, Inst. Astron., ETH Zürich
 ———. 2003, *A&A Rev.*, 11, 153
 Suematsu, Y., et al. 2008, *Sol. Phys.*, in press
 Tritschler, A., & Schmidt, W. 1997, *A&A*, 321, 643
 Weiss, N. O. 2002, *Astron. Nachr.*, 323, 371
 Weiss, N. O., Brownjohn, D. P., Hurlburt, N. E., & Proctor, M. R. E. 1990, *MNRAS*, 245, 434